Investigating decadal variability of El Nino–Southern Oscillation asymmetry by conditional nonlinear optimal perturbation

Wansuo Duan[1] and Mu Mu[1]

Received 26 December 2005; revised 16 April 2006; accepted 3 May 2006; published 19 July 2006.

[1] The observed El Nino events are generally stronger than the La Nina events. This property of El Nino–Southern Oscillation (ENSO) is termed as ENSO asymmetry. Evidence is presented to show that this asymmetry has changed since the famous 1976 climate shift. Along the thinking of how the tropical background field modulates ENSO cycle, we explore the effect of the climatological basic-state change on the ENSO asymmetry by applying the approach of conditional nonlinear optimal perturbation (CNOP) in a theoretical coupled model. CNOP is the initial anomaly pattern that evolves into ENSO event most probably. Observation shows that from the preshift (1961–1975) to the postshift (1981–1995) period, significant changes have occurred in climatological background state, i.e., the mean temperature difference between the equatorial eastern and western Pacific basins and between the mixed-layer and subsurface-layer water, which control the ENSO oscillation in the theoretical coupled model. By computing the CNOPs of the climatological basic state corresponding to the 1961–1975 (1981–1995) epoch, we reproduce the observed decadal change of ENSO asymmetry qualitatively. On the basis of the physics described by the model, the mechanism of ENSO asymmetry change in interdecadal scale is explored in depth. It is shown that the decadal change of ENSO asymmetry is induced by the change of nonlinear temperature advection, which is closely related to the decadal change of the tropical background state. These indicate that the decadal change of ENSO asymmetry results from the collective effect of the changes of the tropical background state and the nonlinearity. These findings in this study also suggest that the nonlinearity can explain not only the asymmetry of interannual ENSO, but also that of interdecadal ENSO, which may present a powerful evidence to the ENSO chaotic theory.

Citation: Duan, W. S., and M. Mu (2006), Investigating decadal variability of El Nino–Southern Oscillation asymmetry by conditional nonlinear optimal perturbation, *J. Geophys. Res.*, *111*, C07015, doi:10.1029/2005JC003458.

1. Introduction

[2] A number of properties (period, amplitude, structure, and propagation) of ENSO have changed since the 1976 climate shift, which is referred to the decadal variation of El Nino-Southern Oscillation (ENSO). Decadal variability is a fundamental characteristic of ENSO oscillation. Many papers have been presented to investigate the decadal ENSO and the associated mechanism [*Zebiak and Cane*, 1991; *McCreary and Lu*, 1994; *Liu et al.*, 1994; *Wang*, 1995; *Gu and Philander*, 1995; *Kleeman et al.*, 1999; *Kleeman and Moore*, 1999; *Wang and An*, 2002]. In these studies, one crucial issue is how the variation of the tropical background state modulates ENSO [*Wang and An*, 2002; *Wang*, 1995; *Gu and Philander*, 1995]. Along this line of thinking, *Wang* [1995] explored the place of initiation of ENSO warming and the propagation through changes in the surface winds and temperature. *Gu and Philander* [1995] emphasized the role of secular changes of the equatorial thermocline in ENSO decadal variability. Recently, *Wang and An* [2002] explained why El Nino properties had changed in a coherent manner since the late 1970s. They further emphasized the role of the tropical background surface wind and the associated upwelling.

[3] What is discussed in this paper is ENSO asymmetry, which is another important characteristic of ENSO oscillation and characterized by the fact that the observed El Nino events are stronger than La Nina events. Observation shows that ENSO asymmetry underwent a significant decadal change (the details are described in section 2) when the properties of ENSO changed from 1961–1975 to 1981–1995 epoch in a coherent manner [*Wang and An*, 2002]. Attention has been paid to the studies of the ENSO asymmetry. *An and Jin* [2004] and *Duan et al.* [2004] investigated the ENSO asymmetry and the associated mechanism and demonstrated that this asymmetry of ENSO is a typical nonlinear property of coupled ocean-atmosphere system. *Jin et al.* [2003] and *An and Jin* [2004] found that the degrees of ENSO asymmetry are significantly different

[1]LASG, Institute of Atmospheric Physics, Chinese Academy of Sciences, Beijing, China.

0148-0227/06/2005JC003458

for the different amplitudes of 1982/1983 and 1997/1998 ENSO events. They argued that it is due to the varying degree of nonlinearity related to ENSO events. Nevertheless, in this paper, the main concern is the decadal variability of ENSO asymmetry. A number of questions should be addressed: what mechanism causes the decadal change of ENSO asymmetry? and what roles do the nonlinearity [*An and Jin*, 2004] and the tropical background state [*Wang and An*, 2002; *Gu and Philander*, 1995] play in decadal change of ENSO asymmetry?

[4] The present study aims to address the above questions using a simple nonlinear ENSO model. To study the decadal behavior of ENSO asymmetry, we will use the approach of conditional nonlinear optimal perturbation (CNOP) in this theoretical ENSO model. CNOP is a new approach to studying climate predictability dynamics proposed by *Mu et al.* [2003], which has been applied to investigate the dynamics of ENSO predictability [*Duan et al.*, 2004] and the sensitivity of ocean thermohaline circulation to finite-amplitude perturbations [*Mu et al.*, 2004], as well as the passive variability of the thermohaline circulation [*Sun et al.*, 2005]. These studies illustrate that CNOP is one of the useful tools for the studies of predictability dynamics and can reveal the effect of nonlinearity on climate predictability. For readers convenience, we will briefly review the ideas of CNOP in section 2.

2. Model and Method

2.1. Theoretical ENSO Model

[5] With a number of simplifications, *Wang and Fang* [1996] (hereafter referred to as WF96) distilled *Zebiak and Cane*'s [1987] intermediate coupled ocean-atmosphere model to a theoretical model. This model consists of only two time-dependent ordinary equations: one describing the evolutions of the anomalous SST T in the equatorial eastern Pacific and the other depicting those of the anomalous thermocline depth h.

$$\begin{cases} \dfrac{dT}{dt} = a_1 T - a_2 h + \sqrt{\dfrac{2}{3}} T(T - \mu h), \\ \dfrac{dh}{dt} = b(2h - T), \end{cases} \tag{1}$$

where $a_1 = (\bar{T}_z + \bar{T}_x - \alpha_s)|_{x_E}$, $a_2 = \mu + \bar{T}_x|_{x_E}$, $b = (2\alpha)/(p(1(p(1 - 3\alpha^2))$, and $p = (1 - H_1/H)(L_0/L_s)^2$. For simplicity, the horizontal advection of temperature is neglected because they have a qualitatively similar effect as that of the vertical temperature advection (WF96). The linear terms in the T-Eq describe the vertical advection by the anomalous upwelling of the mean ocean temperature ($\bar{T}_z T$) and the vertical advection by the mean upwelling of the anomalous ocean temperature ($\bar{T}_x(T - \mu h)$), and the linear damping ($-\alpha_s T$). The coefficients a_1 and a_2 involve basic state parameters $\bar{T}_x$ and $\bar{T}_z$, which characterize, respectively, the mean temperature difference between the equatorial eastern and western basins and between the mixed-layer and subsurface-layer water. These basic state parameters can be time-dependent, reflecting the climatological annual cycle of the basic state. The quadratic term in T-Eq comes from the nonlinear temperature advection by anomalous upwelling of the anomalous temperature. This term represents the nonlinear coupling between surface layer thermodynamics and upper ocean dynamics (thermocline depth fluctuations). The linear terms in h-Eq depict respectively, the effect of equatorial waves on thermocline adjustment ($2bh$) and the effect of the wind forcing ($-bT$). Two nondimensional coupling parameters are presented in this model. One is the air-sea coupling coefficient, α, the other is μ, which measures the degree of coupling between thermocline fluctuation and SST. The meanings and the typical values of the other parameters were listed in Table 1 of WF96 and *Wang et al.* [1999].

[6] The steady solution $O(0, 0)$ of WF96 model represents the climatological mean equilibrium state (including annul cycle) in which both SST and the depth of thermocline are normal. To numerically solve this model, the scheme of fourth-order Runge-Kutta with the time step $dt = 0.01$ (representing one day) is used.

2.2. Conditional Nonlinear Optimal Perturbation

[7] Let M_τ be the propagator of a nonlinear model from 0 to τ. u_0 is an initial perturbation superposed on the basic state $U(t)$, which is a solution to the nonlinear model and satisfies $U(t) = M_t(U_0)$ (U_0 is the initial value).

[8] For a chosen norm $\| \cdot \|$, an initial perturbation $u_{0\delta}$ is called CNOP, if and only if

$$J(u_{0\delta}) = \max_{\|u_0\| \le \delta} \| M_\tau(U_0 + u_0) - M_\tau(U_0) \|,$$

where $\|u_0\| \le \delta$ is constraint condition of initial perturbations defined by norm.

[9] CNOP is the initial perturbation whose nonlinear evolution attains the maximal value of the functional J at time τ [*Mu et al.*, 2003; *Mu and Duan*, 2003]. That is to say, CNOP is the global maximum of the objective function J. But there exists possibility that the objective function J attains its local maximum in a small neighborhood of a point in the phase space. Such initial perturbation is called local CNOP. CNOP and local CNOP possess clear physical meanings. For example, in an anomaly model for ENSO, CNOP (local CNOP) superposed on the climatological background state is most likely to evolve into El Nino (La Nina) event and acts as the optimal precursors of El Nino (La Nina) [*Duan et al.*, 2004]. CNOP and local CNOP can be computed by using sequential quadratic programming (SQP) solver, which is used to solve the nonlinear minimization problems with equality or/and inequality constraint condition [*Powell*, 1982]. The simple description of the algorithm is referred to *Duan et al.* [2004, Appendix].

[10] Although linear theory of singular vector (SV) has been widely applied to address the questions on the ENSO predictability dynamics [*Moore and Kleeman*, 1996; *Thompson*, 1998; *Samelson and Tziperman*, 2001], linear singular vector (LSV) is always associated with the sufficiently small initial perturbation and tangent linear model (TLM) and cannot disclose the effect of nonlinearity on ENSO cycles [*Mu et al.*, 2003; *Mu and Duan*, 2003; *Duan et al.*, 2004]. ENSO asymmetry shows the typical nonlinear characteristic of ENSO oscillation [*An and Jin*, 2004; *An*, 2004], so it is of limitation to use LSV to study the decadal behavior of ENSO nonlinear asymmetry. CNOP is directly

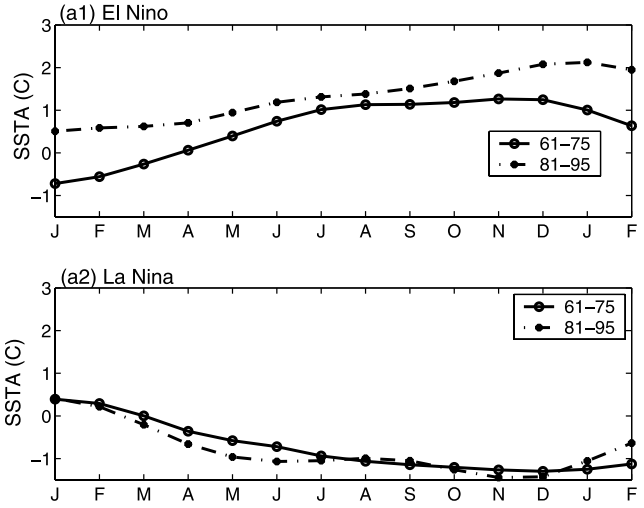

Figure 1. The composite El Nino and La Nina with SODA data. (a1) The composites of El Nino events during 1961–1975 (solid line) and during 1981–1995 (dot-dashed line) epoches, respectively; (a2) the case of La Nina. The SSTA are averaged over Nino-3 region.

from the full nonlinear model without any approximation, by which the ENSO asymmetry in interannual scale has been demonstrated in *Duan et al.* [2004]. It is expected that CNOP can also be used to reveal the decadal variability of ENSO asymmetry.

3. Changes of ENSO Asymmetry Before and After the Late 1970s in the Simple Ocean Data Assimilation Data Set

[11] The dominant ENSO oscillation period increased from 2–3 years during 1961–1975 to 4–6 years during 1981–1995 [*Gu and Philander*, 1995; *Wang and Fang*, 1996]. When the oscillation period increases, the amplitude of El Nino tends to increase as well [*An and Wang*, 2000]. Then, how does the asymmetry of ENSO change?

[12] A simple ocean data assimilation (SODA) data set [*Carton et al.*, 2000] covering a period from 1958.1–2000.12 is used to investigate the asymmetry of interdecadal ENSO. This data set has been checked to be qualified by *An and Jin* [2004]. The SODA data consist of the same variables as NCEP reanalysis data. The latitude and longitude range respectively from 75.25S to 89.25N by 0.5 and from 0.25E to 359.75E by 0.5. The vertical resolution is about 10 m in the upper ocean.

[13] We take respectively the ensemble mean of the SSTA time series corresponding to the El Nino (La Nina) events during 1961–1975 and 1981–1995 epoches and produce respectively the composite of El Nino (La Nina) for the two periods (Figure 1). Note that for the El Nino (La Nina) events during these two periods, we only concern the time series that the SSTA being larger (smaller) than $0.5^{\circ}C$ ($-0.5^{\circ}C$) persists for at least six months, which is generally regarded as the precondition of El Nino (La Nina) onset. For the time period of ENSO shown in Figure 1, we choose 12 months preceding the peak of ENSO and the succeeding two months. Since we only consider the amplitude of El Nino (La Nina), for those that the peak does not phase-lock at December, we move their peaks to December. Comparison of the composite El Nino (La Nina) events during these two periods demonstrates that the composite El Nino event during 1981–1995 years is significantly stronger than that during 1961–1975, while the amplitudes of the composite La Nina events during these two decades are not obviously different. As a result, the asymmetry of ENSO events during 1981–1995 tends to be more considerable than that during 1961–1975 (Figure 2). This indicates that the ENSO asymmetry occurs a significant decadal change accompanying by the variation of ENSO amplitude. *An* [2004] also investigated the asymmetry of ENSO by analyzing the interdecadal change in the skewness of SSTA in the tropical Pacific. Here, we emphasize that the change of ENSO asymmetry is due to the strengthen of the interdecadal El Nino amplitude (see Figures 1 and 2). In the rest of this paper, we will propose a possible mechanism of ENSO asymmetry change by applying the approach of CNOP in the theoretical WF96 ENSO model.

4. Change of Asymmetry in WF96 Model

[14] WF96 used the simplified ENSO model (including an annual cycle) to explain the cyclic, chaotic, and seasonal-dependence evolution of ENSO. In the presence of the basic state annual cycle, WF96 demonstrated that the solution of the dynamical system represents a strange attractor around a stable limit cycle in the phase plane; the corresponding solution in physical space represents an interannual oscillation with inherent deterministic chaos. Furthermore, it is shown that the model ENSO cycle is phase-locked to the basic state seasonal cycle. Recently, *Duan et al.* [2004]

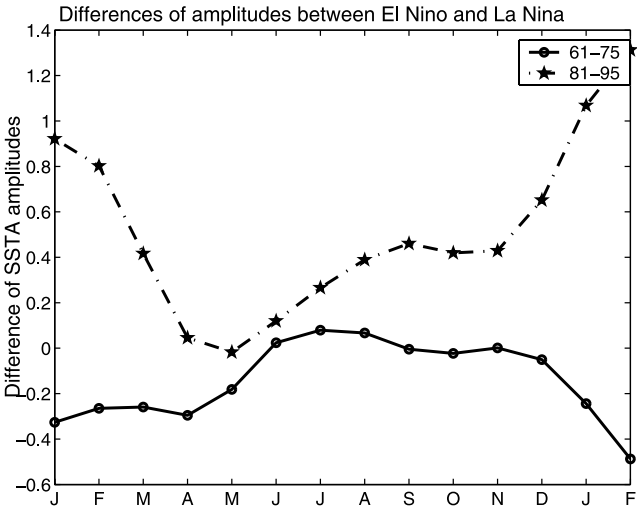

Figure 2. Difference between the composite El Nino and La Nina in term of SSTA amplitude. The line 61–75 (81–95) illustrates the amplitude difference between El Nino and La Nina during 1961–1975 (1981–1995). The values denoted by the line 81–95 are larger than those denoted by the line 61–75, showing that the asymmetry of El Nino and La Nina during 1981–1995 is stronger than that during 1961–1975.

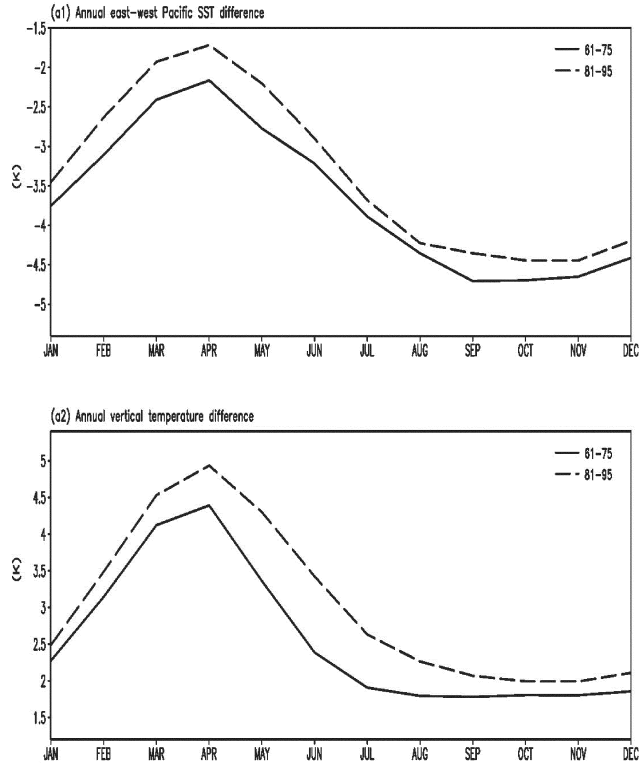

Figure 3. Basic-state annual cycle of the temperature differences (a1) between equatorial eastern and western Pacific and (a2) between mixed layer (5 m) and subsurface layer (57 m) water for the 1961–1975 (solid line) and 1981–1995 (dashed line) periods, respectively.

further demonstrated the asymmetry of El Nino and La Nina by this model. The WF96 model captures the essence of the nonlinear coupling between the surface layer thermodynamics and the upper ocean dynamics and some essential features of the observed ENSO, which therefore provides a convenient tool for analyzing the physics of essential dynamics for ENSO asymmetry.

[15] To examine the physics of decadal variability of ENSO asymmetry, we are along the thinking of how the variation of the tropical background state modulates ENSO to perform the numerical experiments. In WF96 model, the basic state parameters $\bar{T}_x$ and $\bar{T}_z$ control the ENSO dynamics, which represent respectively the mean temperature differences between the equatorial eastern and western Pacific and between the mixed-layer and subsurface-layer water (see section 2). To describe the secular changes in the climatological basic states of tropical Pacific between 1961–1975 and 1981–1995, we focus on these two parameters. Figure 3 illustrates the change of basic state parameters from 1961–1975 to 1981–1995 periods. It is shown that the changes in the basic states are characterized by the large $\bar{T}_x$ and $\bar{T}_z$. To investigate how the climatological basic state affects ENSO asymmetry and maintain the coupled oscillation in the model, we specify the model basic-state parameters $\bar{T}_x$ and $\bar{T}_z$ for 1961–1975 (1981–1995) epoch by averaging the original basic state in WF96 model (see Figure 1 of WF96) and the derived basic state from SODA for 1961–1975 (1981–1995) period.

[16] It has been demonstrated that the CNOP (local CNOP) of the basic-state annual cycle is most likely to evolve into El Nino (La Nina) event and plays the role of optimal precursor of El Nino (La Nina) [*Duan et al.*, 2004]. To investigate the decadal change of ENSO asymmetry, we compute the CNOPs of WF96 model with these above two sets of basic states and make a comparison of the ENSO events derived from CNOPs of 1961–1975 and 1981–1995 basic-states.

[17] Let u_0 be an initial anomaly, we define the nonlinear optimization problem:

$$J(u_{0\delta}) = \max_{\|u_0\| \le \delta} |T(\tau)|,$$

where $T(\tau)$ is the evolution of model SSTA and obtained by integrating WF96 model from 0 to τ. Thus, $J(u_{0\delta})$ describes the maximum evolution of SSTA at prediction time τ. By solving this optimization problem, the optimal initial perturbation satisfying the constraint condition $\|u_0\| \le \delta$, $u_{0\delta}$, can be found. Here, we use the norm $\|u_0\| = \sqrt{T_0 + h_0}$ to define the constraint condition.

[18] For the two sets of basic-state parameters representing 1961–1975 and 1981–1995 periods, the CNOPs (local CNOPs) are respectively calculated for the time interval τ = 12 months with initial time being January. It is shown that there exist a CNOP $u^g_{0\delta}$ and a local CNOP $u^l_{0\delta}$ of the 1961–1975 (1981–1995) basic-state for the constraint condition $\|u_0\| \le \delta$, $\delta \in [0.06, 0.24]$, respectively. For example, for δ = 0.24, the CNOPs of 1961–1975 and 1981–1995 basic-states are respectively (−0.1061, 0.2153) and (−0.1198,0.2080), the local CNOPs of these two basic states are respectively (0.1056, −0.2154) and (0.1421, −0.1934). These CNOPs and local CNOPs are all located on the boundary of the constraint disk $\|u_0\| \le \delta$ and have the most potential to evolve into El Nino and La Nina events respectively. Here, the patterns of CNOP (local CNOP) describe the configuration of the initial anomalies that evolve into El Nino (La Nina) most probably. The two real numbers in CNOP (local CNOP) pattern represent respectively the magnitudes of the nondimensional SSTA (T) and thermocline depth anomaly (h). That is to say, the pattern of negative (positive) SSTA and positive (negative) thermocline depth anomaly acts as the optimal precursor of El Nino (La Nina) [*Duan et al.*, 2004]. In Figures 4 (6), we plot the SSTA components of the evolutions of CNOP (local CNOP) with δ = 0.24 for the two sets of basic-states. The results demonstrate that the El Nino event induced by the CNOP of 1981–1995 basic state are aggressively stronger than that of 1961–1975 basic state, while the La Nina events with these two basic states are trivially different in amplitude. As a result, the derived El Nino and La Nina events with the 1981–1995 basic-state are of the stronger asymmetry than those with the 1961–1975 basic-state. These indicate that the El Nino-La Nina asymmetry occurs decadal change accompanied by the El Nino amplitude change. Similar to the results of SODA, we emphasize that the decadal change of ENSO asymmetry in WF96 model results mainly from the strengthen of El Nino event in interdecadal scale. These theoretical results are consistent

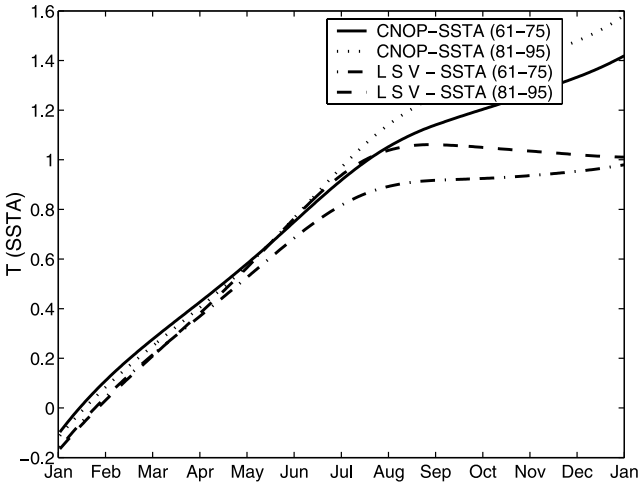

Figure 4. El Nino events induced by CNOPs and the corresponding LSVs, respectively. The lines represent respectively the SSTA evolutions of the CNOPs of 1961–1975 (solid line) and 1981–1995 (dot line) basic states, and those of LSVs of 1961–1975 (dot-dashed line) and 1981–1995 (dashed line). Here, the magnitudes of these initial anomalies in terms of the chosen norm is 0.24.

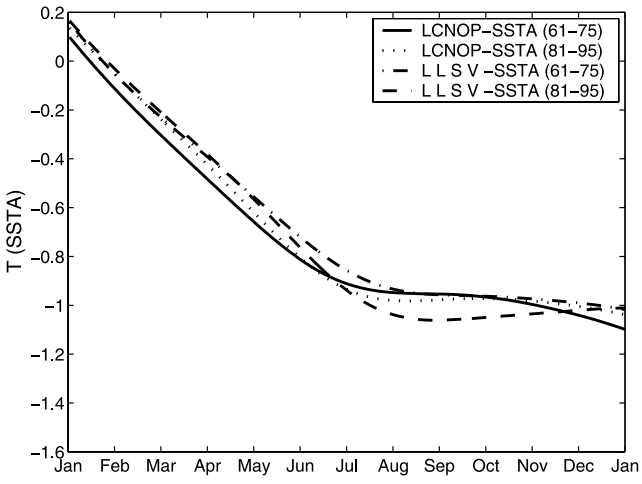

Figure 6. La Nina events induced by local CNOPs and the corresponding LSVs. The lines correspond to the SSTA evolutions of the local CNOPs of 1961–1975 (solid line) and 1981–1995 (dot line) basic states, and those of the corresponding LSVs of 1961–1975 (dot-dashed line) and 1981–1995 (dashed line). These anomalies are of the same magnitudes as those in Figure 4.

with those obtained by SODA in section 3, which has the implication that the decadal change of ENSO asymmetry occurred in observation can be reproduced qualitatively in WF96 model by changing the climatological basic state. It is therefore derived that the decadal change of ENSO asymmetry is closely linked with the variation of tropical background state, i.e., the variation of the mean temperature difference between eastern and western Pacific and between surface-layer and subsurface-layer water.

[19] Besides, it is noticed that during the leading several months of the year in Figure 4, the El Nino events induced by CNOPs of the two sets of basic states are trivially different, even though the two basic states show large differences during this period as shown in Figure 3. That is to say, the ENSO amplitude behaviors a delaying response to the variation of the climatological basic-state parameters $\bar{T}_x$ and $\bar{T}_z$. This indicates that the effect of the climatological basic state on ENSO amplitude could not be a transient response in this model.

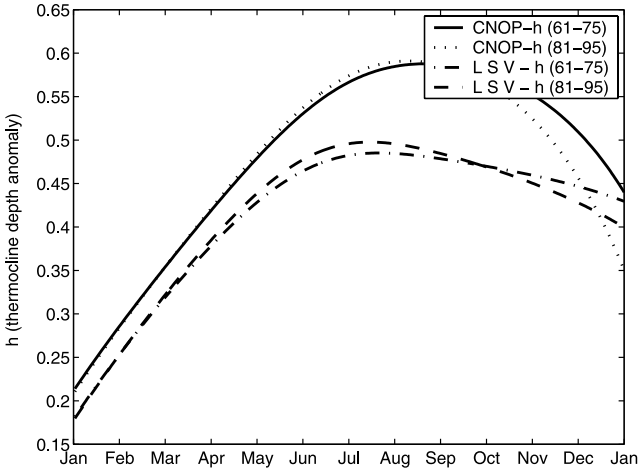

Figure 5. The evolutions of model variable h (thermocline depth anomaly) corresponding to El Nino events induced by CNOP and LSV in Figure 4, respectively.

[20] For the model variable h corresponding to the above CNOP and local CNOP, we also investigate the evolutions (Figures 5–7). It is shown that the mature phase of thermocline displacement h is about 3–4 months ahead of SST mature phase in Figures 4 and 6. After the mature phase of thermocline depth anomaly, the decaying phase leading of the thermocline displacement to SST variation levels off the growing El Nino and provides an negative feedback that drives SSTA to mature phase and further turns the coupled system from warming to cooling or vice. Furthermore, when an ENSO phase turns from warming (cooling) to cooling (warming), the pattern of positive (negative) SSTA and negative (positive) thermocline depth anomaly emerges robustly, which are qualitatively the pattern of local CNOP (CNOP) [*Duan et al.*, 2004]. This implies that the transition phase of thermocline displacement leads the SST transition. These relations between SSTA and thermocline depth anomaly in this model matures qualitatively the observation and supports the results of WF96 and *Duan et al.* [2004] (see Figure 8 in WF96 and Figures 9 and 10 in *Duan et al.* [2004]).

[21] Now we turn to investigate the role of nonlinearity in the decadal change of ENSO asymmetry. To achieve it, we compare the results of CNOP with those of LSV. The anomaly pattern $u_{0L}^{1}(-0.0209,0.0224)$ and $u_{0L}^{2}(-0.0220, 0.0213)$ are respectively a LSV of the 1961–1975 and 1981–1995 basic states, which are the fastest growing perturbations of the TLM of WF96 model with respect to the two sets of climatological states, respectively. To facilitate the discussion, we define the scaled LSVs for

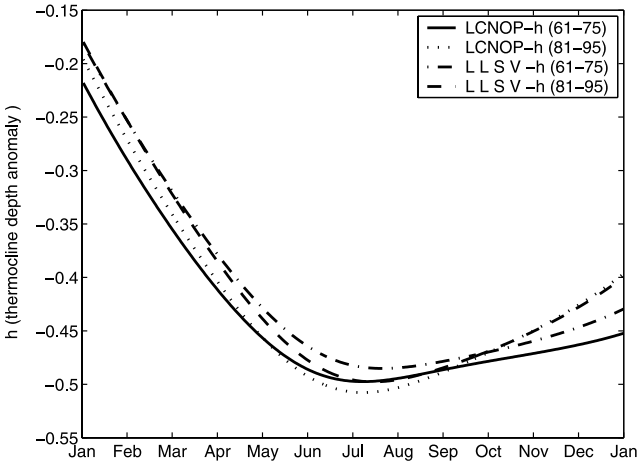

Figure 7. The evolutions of model variable h (thermocline depth anomaly) corresponding to La Nina events induced by local CNOP and LSV in Figure 5, respectively.

the 1961–1976 (1981–1995) basic-state in the following manner:

$$u_{0L}^{E} = \frac{\| u_{0\delta}^{E} \|}{\| u_{0L} \|} u_{0L}, \qquad u_{0L}^{l} = -\frac{\| u_{0\delta}^{l} \|}{\| u_{0L} \|} u_{0L}$$

$$\| u_{0L}^{E} \| = \| u_{0L}^{l} \| = \| u_{0\delta}^{E} \| = \| u_{0\delta}^{l} \| = \delta,$$

where u_{0L} represents the LSV u_{0L}^{1} (u_{0L}^{2}) with $\delta = 0.24$ for 1961–1976 (1981–1995) basic-state. Note that the scaled LSVs u_{0L}^{E} and u_{0L}^{l} for the 1961–1975 (1981–1995) basic state also evolve into an El Nino and a La Nina events in TLM of WF96 model respectively (Figures 4 and 6). But the El Nino events obtained by TLM and LSV are considerably weaker than those derived by CNOP for each basic state, while the La Nina events resulted from LSV and local CNOP do not have significant difference, then resulting in the asymmetry of ENSO [*Duan et al.*, 2004]. These indicate that the nonlinearity determines the asymmetry of ENSO, which also shed light on that the El Nino and La Nina obtained by the scaled LSVs are symmetric in TLM due to the absence of nonlinear term. And this linear symmetry of ENSO remains unchanged in TLM with the basic state changing from 1961–1975 to 1981–1995 parameters, although the ENSO amplitude occurs an obvious change in TLM by changing the basic state. The nonlinear asymmetry of El Nino and La Nina derived by CNOP and local CNOP occurs a considerable change from 1961–1975 to 1981–1995 basic-states (Figure 8). All these have the implication that the decadal change of ENSO asymmetry is associated with the nonlinearity. *An and Jin* [2004] also realized the role of nonlinearity. In WF96 model, this nonlinearity comes from the nonlinear temperature advection and represents the nonlinear coupling between surface layer thermodynamics and upper ocean dynamics. Hence, it can be reasonably told that the nonlinear temperature advection plays a decisive role in the decadal change of ENSO asymmetry occurred in WF96 model.

[22] The asymmetry of ENSO is a typical nonlinear property of ENSO oscillation. The nonlinear term of WF96 model, $\eta(T, h) = \sqrt{\frac{2}{3}}T(T - a_3 h)$, enhances El Nino and affects (suppresses) negligibly La Nina and leads to the asymmetry of ENSO. From the first equation of the WF96 model, it is easily shown that the larger the nonlinear term $\eta(T, h)$, the more considerable the strengthen of El Nino, then the more significant the asymmetry of ENSO. Note that, the nonlinear term $\eta(T, h)$ depends on the involved ENSO events. For the two sets of basic states, the amplitudes of the derived ENSO events are different. Correspondingly, the associated nonlinear terms amplitudes are also in difference (Figures 9 and 10). Practically, with the basic state changing from 1961–1975 to 1981–1995 parameters, the nonlinear term $\eta(T, h)$ increases, which is accompanied by the ENSO amplitude change. Consequently, the El Nino is much strengthened by the increasing nonlinearity. Although the magnitude of the nonlinear term corresponding to La Nina is also increased positively, it is relatively quite small and can be neglected. Then the suppression of the La Nina by nonlinearity is negligible. Thus, the strengthening El Nino induces the more considerable asymmetry of ENSO in interdecadal scale.

[23] The El Nino event is also strengthened in TLM by changing basic state parameters, but the TLM is absent of the nonlinear term. And the El Nino events cannot therefore be further enhanced by positive nonlinear term. In this situation, El Nino and La Nina in TLM keep the same amplitude due to the linearity, i.e., they are symmetric. These also emphasize the important role of the nonlinearity, which triggers the asymmetry of ENSO. As for the magnitude of nonlinear term corresponding to La Nina being significantly smaller than that of El Nino, it has a simple

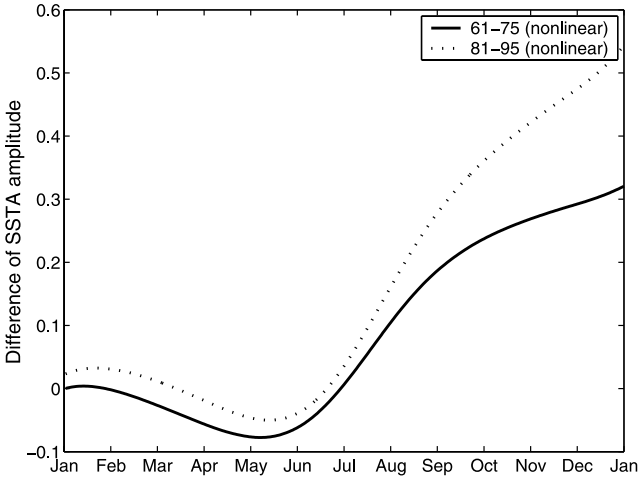

Figure 8. Amplitude differences between El Nino and La Nina in WF96 model, where the amplitude is measured by the absolute of SSTA. The solid (dot) line denotes the amplitude differences between El Nino and La Nina, which are respectively induced by the same magnitude of CNOP and local CNOP as in Figures 4 and 5.

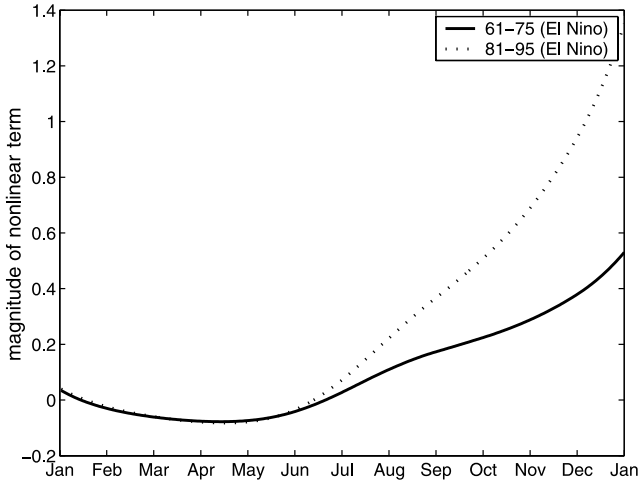

Figure 9. Magnitude of nonlinear term associated with El Nino induced by CNOP with $\delta = 0.24$ as a function of the time t, which is derived by integrating WF96 model with CNOP as initial value. The solid (dot) line denotes the nonlinear term ($\eta(T, h)$) with basic-state 1961–1975 (1981–1995).

discussion. During an El Nino, when the SSTA evolves to be large, the warming in the eastern Pacific increases anomalous vertical temperature difference across the mixed layer base, $T - T_e = T - \mu h$ (where T_e denotes the entrained water temperature from beneath the mixed layer) [*Wang et al.*, 1999]. The $T - T_e$ is largely greater than normal and much favorable for the strengthen of nonlinear temperature advection $\eta(T, h) = T(T - \mu h)$ induced by the downwelling of the anomalous temperature in equatorial eastern Pacific. In this situation, the largely largening nonlinear term $\eta(T, h)$ enhances aggressively the El Nino. For the La Nina events, the sufficient cooling decreases the anomalous vertical temperature difference ($T - T_e$) in equatorial Pacific, which induces the trivial offset (or suppression) of the contribution of anomalous upwelling to SST cooling by $\eta(T, h)$ in this model [*Wang et al.*, 1999; *Duan et al.*, 2004]. Then the effect of this offset (suppression) on La Nina is relatively quite small compared to the enhancing of El Nino by nonlinear temperature advection induced by anomalous upwelling (here is downwelling) of the anomalous temperature, which may interpret why the magnitude of nonlinear term corresponding to La Nina is significantly smaller than that of El Nino. Actually, these discussions are based on the above theoretical model. It is expected that they are also tenable in a realistic ENSO model.

[24] The above discussions demonstrate that the decadal change of ENSO asymmetry is associated with not only the variations of the tropical background state, but also the nonlinear temperature advection. The anomalously large mean temperature differences between the equatorial eastern and western basins and between the mixed-layer and subsurface-layer water induce the anomalously strong ENSO events, which causes the strengthened nonlinear coupling between surface thermodynamics and the upper ocean dynamics, then resulting in the anomalously strong asymmetry of ENSO. These indicate that the changing ENSO asymmetry may result from the collective of the decadal changes of the tropical background state and the nonlinearity related to ENSO oscillation.

5. Summary and Discussion

[25] Comparison of the ENSO events observed during the 1961–1975 and 1981–1995 epoches reveals that the degree of El Nino-La Nina asymmetry has occurred an obvious decadal change due to the strengthen of El Nino amplitude. A considerable change is also found in the climatological background state - the mean temperature differences between eastern and western equatorial Pacific basins ($\bar{T}_x$) and between surface-layer and subsurface-layer water ($\bar{T}_z$), which control the ENSO oscillation in the theoretical coupled model of *Wang and Fang* [1996] (WF96). These two basic-state parameters have been dominated by the anomalously large $\bar{T}_x$ and $\bar{T}_z$ since the late 1970s.

[26] The WF96 coupled model is used to explore the physics of ENSO asymmetry change. By a new approach of conditional nonlinear optimal perturbation (CNOP), the nonlinearity of ENSO asymmetry and its decadal variability is demonstrated. In these explorations, we first reproduce the decadal change of ENSO asymmetry by changing the tropical background states in WF96 model. This indicates that the change of El Nino-La Nina asymmetry may be linked with the decadal variation of the tropical background state $\bar{T}_x$ and $\bar{T}_z$. However, the decadal change of ENSO asymmetry cannot be achieved in the linearized version of the WF96 model. This further has the implication that the nonlinearity play a decisive role in the decadal change of ENSO asymmetry. Hence, the ENSO asymmetry change in interdecadal scale is closely associated with the tropical background state and the nonlinearity. In fact, it results from the collective effect of the tropical background state and the nonlinearity. In this model, the change of the tropical background state induces the strengthened El Nino events,

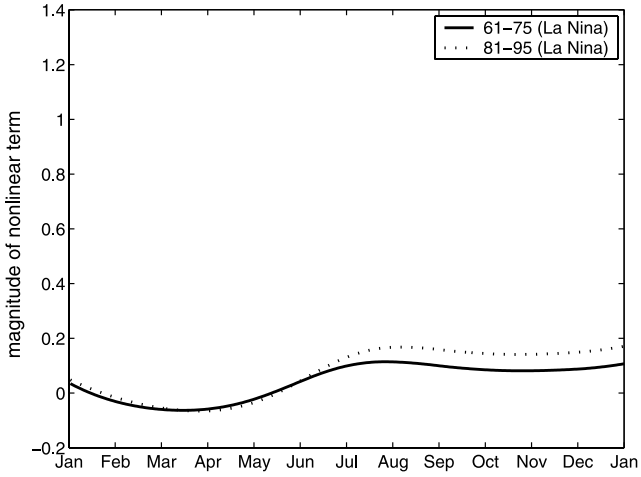

Figure 10. Magnitude of nonlinear term associated with La Nina induced by local CNOP with $\delta = 0.24$ as a function of the time t, which is derived by integrating WF96 model with local CNOP as initial value. The solid (dot) line corresponds to the nonlinear term ($\eta(T, h)$) with basic-state 1961–1975 (1981–1995).

which then results in the change of nonlinear coupling and further leads to the decadal change of ENSO asymmetry. These may provide a possible mechanism of the decadal variation of ENSO asymmetry.

[27] The underlying processes responsible for ENSO irregularity remain controversial. One popular idea is ENSO chaos, which regards ENSO as a result of self sustained oscillation in an unstable nonlinear dynamical system [*Schopf and Suarez*, 1988; *Chen et al.*, 1995, 2004]. Another competing theory views ENSO as a stable linear process driven by stochastic forcing [*Penland and Sardeshmukh*, 1995]. In this study, considering the ENSO asymmetry is closely related to the nonlinearity, the decadal change of ENSO asymmetry may belong to the scenario of nonlinearity. The finding in this study implies that the nonlinearity can reveal the physics of the ENSO asymmetry of not only in interannual scale, but also in the interdecadal scale, which may further present a powerful evidence to the ENSO chaotic oscillation.

[28] These results are derived from a simple theoretical model. The resultant results are qualitatively indicative. Also the data are insufficient and of a crude vertical resolution of the observed subsurface temperature, the results obtained from data analysis are considered suggestive. It is expected that the more accurate observation and more realistic model are obtained to investigate the decadal variability of ENSO, and more significant finds are obtained to serve the prediction of decadal change for ENSO.

[29] **Acknowledgments.** We thank the anonymous reviewers for useful suggestions. We also thank Bin Wang from University of Hawaii for his insightful suggestions. This work was jointly sponsored by the National Nature Scientific Foundation of China (40505013, 40233029, and 40523001), KZCX3-SW-230 of the Chinese Academy of Sciences, and CAS International Partnership Creative Group "The Climate System Model Development and Application Studies."

References

An, S.-I. (2004), Interdecadal changes in the El Nino-La Nina asymmetry, *Geophys. Res. Lett.*, *31*, L23210, doi:10.1029/2004GL021699.

An, S.-I., and F. F. Jin (2004), Nonlinearity and asymmetry of ENSO, *J. Clim.*, *17*, 2399–2412.

An, S.-I., and B. Wang (2000), Interdecadal change of the structure of the ENSO mode and its impact on the ENSO frequency, *J. Clim.*, *13*, 2044–2055.

Carton, J. A., G. Chepurin, X. Cao, and B. Giese (2000), A simple ocean data assimilation analysis of the global upper ocean 1950–95. Part I: methodology, *J. Phys. Oceanogr.*, *30*, 294–309.

Chen, D., S. E. Zebiak, A. J. Busalacchi, and M. A. Cane (1995), An improved procedure for El Nino forecasting, *Science*, *269*, 1699–1702.

Chen, D., M. A. Cane, A. Kaplan, S. E. Zebiak, and D. J. Huang (2004), Predictability of El Nino over the past 148 years, *Nature*, *428*, 733–736.

Duan, W. S., M. Mu, and B. Wang (2004), Conditional nonlinear optimal perturbation as the optimal precursors for El Nino-Southern Oscillation events, *J. Geophys. Res.*, *109*, D23105, doi:10.1029/2004JD004756.

Gu, D., and S. G. H. Philander (1995), Interdecadal climate fluctuations that depend on exchanges between the tropics and extratropics, *Science*, *275*, 805–807.

Jin, F. F., S. I. An, A. Timmermann, and J. X. Zhao (2003), Strong El Nino events and nonlinear dynamical heating, *Geophys. Res. Lett.*, *30*(3), 1120, doi:10.1029/2002GL016356.

Kleeman, R., and A. M. Moore (1999), A new method for determining the reliability of dynamical ENSO prediction, *Mon. Weather Rev.*, *127*, 694–705.

Kleeman, R., J. P. McCreary, and B. A. Klinger (1999), A mechanism for generating ENSO decadal variability, *Geophys. Res. Lett.*, *26*, 1743–1746.

Liu, Z., S. G. H. Philander, and R. C. Pacanowski (1994), A GCM study of the tropical-subtropical upper ocean water exchange, *J. Phys. Oceanogr.*, *24*, 2606–2623.

McCreary, J. P., and P. Lu (1994), Interaction between the subtropical and equatorial ocean circulation: the subtropical cell, *J. Phys. Oceanogr.*, *24*, 466–497.

Moore, A. M., and R. Kleeman (1996), The dynamics of error growth and predictability in a coupled model of ENSO, *Q. J. R. Meteorol. Soc.*, *122*, 1405–1446.

Mu, M., and W. S. Duan (2003), A new approach to studying ENSO predictability: conditional nonlinear optimal perturbation, *Chin. Sci. Bull.*, *48*, 1045–1047.

Mu, M., W. S. Duan, and B. Wang (2003), Conditional nonlinear optimal perturbation and its applications, *Nonlinear Processes Geophys.*, *10*, 493–501.

Mu, M., L. Sun, and D. A. Henk (2004), The sensitivity and stability of the ocean's thermocline circulation to finite amplitude freshwater perturbations, *J. Phys. Oceanogr.*, *34*, 2305–2315.

Peland, C., and P. Sardeshmukh (1995), The optimal growth of tropical sea surface temperature anomalies, *J. Clim.*, *8*, 1999–2004.

Powell, M. J. D. (1982), VMCWD: A FORTRAN subroutine for constrained optimization, *DAMTP Rep. 1982/NA4*, Univ. of Cambridge, Cambridge, U. K.

Samelson, R. G., and E. Tziperman (2001), Instability of the chaotic ENSO: The growth-phase predictability barrier, *J. Atmos. Sci.*, *58*, 3613–3625.

Schopf, P. S., and M. J. Suarez (1988), Vacillations in a coupled ocean-atmosphere model, *J. Atmos. Sci.*, *45*, 549–566.

Sun, L., M. Mu, D. J. Sun, and X. Y. Yin (2005), Passive mechanism of decadal variation of thermohaline circulation, *J. Geophys. Res.*, *110*, C07025, doi:10.1029/2005JC002897.

Thompson, C. J. (1998), Initial conditions for optimal growth in a coupled ocean-atmosphere model of ENSO, *J. Atmos. Sci.*, *55*, 537–557.

Wang, B. (1995), Interdecadal changes in El Nino onset in the last four decades, *J. Clim.*, *8*, 267–285.

Wang, B., and S.-I. An (2002), A mechanism for decadal changes of ENSO behavior: roles of background wind changes, *Clim. Dyn.*, *18*, 475–486.

Wang, B., and Z. Fang (1996), Chaotic oscillation of tropical climate: A dynamic system theory for ENSO, *J. Atmos. Sci.*, *53*, 2786–2802.

Wang, B., A. Barcilon, and Z. Fang (1999), Stochastic dynamics of El Nino-Southern Oscillation, *J. Atmos. Sci.*, *56*, 5–23.

Zebiak, S. E., and A. Cane (1987), A model El Nino-Southern oscillation, *Mon. Weather Rev.*, *115*, 2262–2278.

Zebiak, S. E., and M. A. Cane (1991), Natural climate variability in a coupled model, in *Greehouse Gas Induced Climate Change*, edited by M. E. Schlessinger, pp. 457–470, Elsevier, New York.

W. S. Duan and M. Mu, LASG, Institute of Atmospheric Physics, Chinese Academy of Sciences, Beijing 100029, China. (duanws@lasg.iap.ac.cn)